

Control of Rayleigh-like waves in thick plate Willis metamaterials

André Diatta¹, Younes Achaoui¹, Stéphane Brûlé², Stefan Enoch¹ and Sébastien Guenneau¹

1. Aix–Marseille Univ., CNRS, Centrale Marseille, Institut Fresnel, 13013 Marseille, France

2. Dynamic soil laboratory, Ménard, 91620 Nozay, France

Recent advances in control of anthropic seismic sources in structured soil led us to explore interactions of elastic waves propagating in plates (with soil parameters) structured with concrete pillars buried in the soil. Pillars are 40 m in depth and the plate is 100 m in thickness, so that typical frequencies under study are in the frequency range 4 to 8 Hz, which is compatible with frequency ranges of particular interest in earthquake engineering. It is demonstrated in this paper that two seismic cloaks' configurations allow for an unprecedented flow of elastodynamic energy associated with Rayleigh surface waves. These designs are inspired by some ideal cloaks' parameters deduced from a geometric transform in the Navier equations that preserves the symmetry of the elasticity tensor but leads to Willis' equations as corroborated by numerical simulations. Importantly, we focus our attention on geometric transforms applied to thick plates, which is an intermediate case between thin plates and semi-infinite media, not studied previously. Cloaking effects (reduction of the disturbance of the wave wavefront and its amplitude behind an obstacle) and protection (reduction of the wave amplitude within the center of the cloak) are studied for ideal and approximated cloaks' parameters, the latter being based upon effective medium considerations. These results represent a first step towards designs of seismic cloaks for surface Rayleigh waves propagating in sedimentary soils structured with concrete pillars.

I. INTRODUCTION

In a recent theoretical proposal [1], control of body waves was numerically demonstrated with a spherical shell consisting of an anisotropic heterogeneous elasticity tensor without the minor symmetries (what falls within the framework of so-called Cosserat media), and an heterogeneous (but isotropic) density. In [1], it was suggested that a simplified version of this elastodynamic cloak could be implemented to protect objects, nuclear waste or even large scale infrastructures buried deep down in the soil. However, achieving asymmetric elasticity tensors for instance via effective medium approaches remains a challenge. Indeed, the Cosserat theory [2] of elasticity (or micropolar elasticity) incorporates a local rotation of points as well as the translation assumed in classical elasticity, and a couple stress (a torque per unit area) as well as the force stress (force per unit area). In the isotropic Cosserat solid or micropolar continuum, there are six elastic constants, in contrast to the classical elastic solid which is described by two constants. This makes Cosserat cloaks fairly challenging to engineer. In the present paper, we follow a different route towards seismic wave cloaking for surface Rayleigh waves, without resorting to Cosserat media. Before we embark the reader on this journey, we would like to first recall why soils structured at a meter scale might counteract deleterious action of certain types of seismic waves, what might seem at first glance fairly counter-intuitive.

More than a million earthquakes are recorded every year, by a worldwide system of earthquake detection stations, some of which are particularly devastating and cause human casualties, such as the earthquake of magnitude-6.2 that struck Italy on the 22nd of August at 01:36 GMT, 100 km north-east of Rome, not far from L'Aquila, where a similar earthquake struck on the 9th of April 2009. The propagation velocity of the seismic waves depends on density and elasticity of the earth materials (clearly, it is much different in sedimentary soils and rocks). At the scale of an alluvial basin, such as in L'Aquila, seismic effects involve various phenomena, such as wave trapping, resonance of whole basin, propagation in heterogeneous media, and the generation of surface waves at the basin edge [3]. As noted in [4], wherein meter-scale inertial resonators were introduced to reflect surface and body seismic waves, due to the surface wave velocity in superficial and under-consolidated recent material (less than 100 to 300 m.s⁻¹), wavelengths of surface waves induced by natural seismic sources or construction work activities are shorter than those of earthquake generated direct P (primary, i.e. longitudinal compressional) and S (secondary, i.e. transverse shear) waves (considering the 0.1-50 Hz frequency range), from a few meters to a few hundreds of meters. These are of similar length to that of buildings, therefore leading to potential building resonance phenomena in the case of earthquakes such as in L'Aquila. Other sources of soil vibrations one may wish to attenuate include traffic and construction works [5], and screening methods have been proposed to achieve that [6, 7].

Interestingly, back in 1999 Rayleigh wave attenuation was theoretically and experimentally achieved in marble quarry with air holes displaying kHz stop bands [8] and similar filtering effects in a microstructured piezoelectric for MHz till 1 GHz surface waves [9–12]. In our previous work on control of surface Rayleigh waves in soils structured with borehole inclusions, we used so-called elastic stop bands which are frequency intervals for which waves are disallowed to propagate in an infinite periodic array through Bragg interferences (when the wave wavelength is on the order of the array pitch). With boreholes 0.3m in diameter, with a center to center spacing of 1.7m and the soil parameters

on this field experiment [13], this meant we had a stop partial band around 50 Hz (for only one crystallographic direction). Three rows of boreholes were enough to reduce the energy of the signal by about 30 per cent behind the seismic metamaterial. However, if one were to design a shield for the frequency interval 5 to 10 Hz, it would be necessary to scale up the array of boreholes by a factor of five to ten, which requires a lot of free space around the area, one wishes to protect. To overcome this obstacle, we now propose to use columns of concrete instead of boreholes, so as to achieve subwavelength control of Rayleigh surface waves. We show in figure 1 an example of such a structured soil, which was designed by civil engineers of the Ménard company.

Importantly, the contrast between the soil and concrete column's parameters makes it possible to achieve uncommon effective material parameters, such as with strong artificial anisotropy and dispersion, and even artificial inertia and viscosity that can be interpreted as rank-3 tensors in an effective Willis equation. This leads to a markedly enhanced control of surface Rayleigh wave trajectories compared to our earlier work [13]. Indeed, comparisons between numerical results demonstrate that one can achieve some cloaking of surface (Rayleigh-like) wave trajectories, where the wave field is almost unperturbed outside the seismic cloak, whereas it nearly vanishes in its center. Bearing in mind that we use soil and concrete elastic parameters for the thick plate and pillars, and that we consider wave frequencies lower than 10 hertz, we claim that our results represent a preliminary step towards implementation of seismic cloaks in civil engineering.

In this paper, we would like to present a novel approach for the design of seismic cloaks, which is based on the Willis-type equations, as proposed in the seminal paper by Milton, Briane and Willis [14], which investigated form invariant governing equations in physics, notably coordinates transforms in Navier equations ensuring a transformed symmetric elasticity tensor. For the sake of simplicity in the numerical computations and physical discussions, we shall restrict ourselves to elastic waves in thick plates, rather than in semi-infinite media. However, we consider wavelengths small compared to the plate's thickness, hence surface waves are akin to Rayleigh, rather than Lamb, waves. Indeed, as noted in [13], the elastic plate model already gives some interesting insight in the physics of seismic waves. The plan of the paper is as follows: We first present some derivation of transformed Navier equations with a symmetric elasticity tensor, for thick plates. The obtained Willis equations are then simplified (removal of rank-3 tensors) and the illustrative case of a cloak with heterogeneous anisotropic Willis equations is numerically solved with finite elements implemented in the COMSOL commercial package. We then explain how one can approximate these anisotropic elastic parameters with an effective medium approach. The touchstone of our homogenization approach is that all tensors are symmetric. We finally propose two designs of soils structured with concrete pillars which are numerically validated with finite elements. We show in figure 1 a typical field test experiment by the Ménard company that could serve as a basis for the validation of our concept of seismic cloak.



Figure 1: Photo of a soil reinforced with columns of concrete 0.4m in diameter and 15m in depth (Courtesy of Ménard).

II. ELASTODYNAMIC WILLIS MATERIAL, EQUATIONS OF MOTION

The propagation of elastic waves is governed by the Navier equations. Assuming time harmonic $\exp(-i\omega t)$ dependence, with ω as the angular wave frequency and t the time variable, allows us to work directly in the spectral domain.

Such dependence is assumed henceforth and suppressed, leading to

$$\nabla \cdot \boldsymbol{\sigma} = -i\omega \mathbf{p}, \quad \boldsymbol{\sigma} = \mathbb{C} : \nabla \mathbf{u}, \quad \mathbf{p} = -i\omega \rho \mathbf{u}, \quad (1)$$

where ρ is the density of the (possibly heterogeneous isotropic) elastic medium and $\mathbf{u} = (u_r, u_\theta, u_z)$ is the three-component displacement field in a cylindrical coordinate basis $\mathbf{x} = (r, \theta, z)$. Also, \mathbb{C} is the rank-four (symmetric) elasticity tensor with components C_{ijkl} ($i, j, k, l = r, \theta, z$) and $:$ stands for the double contraction between tensors. For example, $\mathbb{C} : \nabla \mathbf{u}$ is the 2-tensor with components $(\mathbb{C} : \nabla \mathbf{u})_{ij} = C_{ijkl} (\nabla \mathbf{u})_{kl}$. Let us consider a coordinate change $\mathbf{x} \mapsto \mathbf{x}'$, where $\mathbf{x}' = (r', \theta', z')$ are stretched spherical coordinates. In general, this leads to a transformed equation [14, 15]

$$\nabla' \cdot (\mathbb{C}' : \nabla' \mathbf{u}' + \mathbf{S} \cdot \mathbf{u}') = -i\omega (\mathbf{D} : \nabla' \mathbf{u}' - i\omega \rho \mathbf{u}'), \quad \mathbf{u}' = \mathbf{A}^{-T} \mathbf{u}, \quad (2)$$

or, in a more compact way

$$\begin{aligned} \nabla' \cdot \boldsymbol{\sigma}' &= -i\omega \mathbf{p}', & \boldsymbol{\sigma}' &= \mathbb{C}' : \nabla' \mathbf{u}' + \mathbf{S} \cdot \mathbf{u}', \\ \mathbf{p}' &= \mathbf{D} : \nabla' \mathbf{u}' - i\omega \rho \mathbf{u}', & \mathbf{u}' &= \mathbf{A}^{-T} \mathbf{u}, \end{aligned} \quad (3)$$

where \mathbf{S} , \mathbf{D} are 3-tensor fields, ∇' is the gradient in transformed coordinates \mathbf{x}' and $\mathbf{u}'(\mathbf{x}') = \mathbf{u}'(r', \theta', z')$ is a transformed displacement in stretched cylindrical coordinates. Note that the transformed stress is generally not symmetric. Note also that in general \mathbf{A} is a matrix field. In order to preserve the symmetry of the stress tensor, one assumes that \mathbf{A} is a multiple $\mathbf{A} = \xi \partial \mathbf{x}' / \partial \mathbf{x}$, of the Jacobian matrix $\partial \mathbf{x}' / \partial \mathbf{x}$ of the transformation, where ξ is a non-zero scalar, in which case (2), (3) are said to be Willis-type equations [14, 16].

III. APPROXIMATED CLOAKING WITH WILLIS MATERIAL WITHOUT 3-TENSORS

Following the proposal of Pendry et al. of an invisibility cloak via transformation optics [17], we consider a specific geometric transformation, in cylindrical coordinates

$$r' = \begin{cases} r_1 + \frac{r_2 - r_1}{r_2} r, & \text{if } 0 \leq r \leq r_2 \\ r & \text{if } r \geq r_2 \end{cases} \quad (4)$$

with $\theta' = \theta, z' = z$. Such a transformation blows the axis $\{(r, \theta, z), r = 0\}$ of a vertical solid cylinder of radius r_2 , into the cylinder $\{(r, \theta, z), r = r_1\}$, while confining the whole solid cylinder $\{(r, \theta, z), r \leq r_2\}$ into the following hollow cylinder $\{(r, \theta, z), r_1 \leq r \leq r_2\}$ of inner and outer radii r_1 and r_2 respectively.

In the sequel, we plug the transformation (4) into the Navier equations

$$\nabla \cdot \mathbb{C} : \nabla \mathbf{u} + \rho \omega^2 \mathbf{u} = \mathbf{0}, \quad (5)$$

to derive the corresponding transformed equations (2), (3). From here on, we drop (neglect) the 3-order tensors \mathbf{S} and \mathbf{D} and hence use an approximate version of the Willis-like Equations. Note that in this case, \mathbb{C}' obviously still has its minor and major symmetries, but is anisotropic and heterogeneous, with coefficients in cylindrical coordinates

$$C'_{r'r'r'r'} = \left(\frac{r_2 - r_1}{r_2} \right)^2 \frac{r' - r_1}{r'} (\lambda + 2\mu); \quad C'_{r'r'\theta\theta} = C'_{\theta\theta r'r} = \left(\frac{r_2 - r_1}{r_2} \right)^2 \frac{r'}{r' - r_1} \lambda; \quad (6)$$

$$C'_{r\theta r\theta} = C'_{r'\theta\theta r} = C'_{\theta r r \theta} = C'_{\theta r \theta} = \left(\frac{r_2 - r_1}{r_2} \right)^2 \frac{r'}{r' - r_1} \mu;$$

$$C'_{r r z z} = C'_{z z r r} = \frac{r' - r_1}{r'} \lambda;$$

$$C'_{r z r z} = C'_{r' z z r} = C'_{z r r z} = C'_{z r z r} = \frac{r' - r_1}{r'} \mu;$$

$$C'_{\theta\theta\theta\theta} = \left(\frac{r_2 - r_1}{r_2} \right)^2 \left(\frac{r'}{r' - r_1} \right)^3 (\lambda + 2\mu); \quad C'_{\theta\theta z z} = C'_{z z \theta\theta} = \frac{r'}{r' - r_1} \lambda;$$

$$C'_{\theta z \theta z} = C'_{\theta z z \theta} = C'_{z \theta \theta z} = C'_{z \theta z \theta} = \frac{r'}{r' - r_1} \mu;$$

$$C'_{z z z z} = \left(\frac{r_2 - r_1}{r_2} \right)^2 \frac{r' - r_1}{r'} (\lambda + 2\mu). \quad (7)$$

The stretched density ρ' is now a tensor field of order 2, in particular, it is anisotropic and inhomogeneous. Namely, it has non-constant different eigenvalues and is diagonal in cylindrical coordinates with components as follows

$$\rho' = \text{diag}(\rho'_{r'r'}, \rho'_{\theta\theta}, \rho'_{zz}) = \rho \text{diag}\left(\frac{r' - r_1}{r'}, \frac{r'}{r' - r_1}, \frac{r_2^2}{(r_2 - r_1)^2} \frac{r' - r_1}{r'}\right). \quad (8)$$

Although all the (minor and major) symmetries of \mathbb{C} are preserved, the anisotropy in the azimuthal direction is infinite at the inner boundary of the cloak, as $C'_{\theta\theta\theta\theta}/C'_{r'r'r'r'} = \left(\frac{r'}{r' - r_1}\right)^4$ recedes to infinity as quickly as $\left(\frac{1}{r' - r_1}\right)^4$ when r' approaches r_1 . However $C'_{r'r'r'r'}$ and C'_{zzzz} are of the same order and both tend to zero at the same rate at the inner boundary $r' = r_1$. Meanwhile, at the same boundary, the off-diagonal components $C'_{r'r'\theta\theta}$, $C'_{\theta\theta r'r'}$, $C'_{r'\theta r\theta}$, $C'_{r'\theta\theta r}$, $C'_{\theta r'\theta}$, $C'_{\theta r'\theta}$, $C'_{\theta\theta\theta\theta}$, $C'_{\theta\theta zz}$, $C'_{zz\theta\theta}$, $C'_{\theta zz\theta}$, $C'_{\theta z\theta z}$, $C'_{z\theta\theta z}$, $C'_{z\theta z\theta}$, all become infinite at the rate $\frac{1}{r' - r_1}$, whereas $C'_{r'r'zz}$, $C'_{zzr'r'}$, $C'_{r'zzr'}$, $C'_{r'zzr'}$, $C'_{zr'r'z}$, $C'_{zr'r'z}$, $C'_{\theta zz\theta}$, $C'_{\theta z\theta z}$, $C'_{z\theta\theta z}$, $C'_{z\theta z\theta}$, tend to zero. One remarks in the meantime that, the eigenvalues $\rho'_{r'r'}$ and $\rho'_{z'z'}$ of the density in the r and z directions both vanish, whereas in the azimuthal direction $\rho'_{\theta'\theta'}$ becomes infinite at the inner boundary of the cloak.

1. Rayleigh-like waves in thick plates

In this paper, we apply the approximate Willis cloaking discussed above, to Rayleigh waves in particular in the framework of seismic metamaterials. Rayleigh waves, unlike Love waves, are surface waves that do not need a layer to guide them. The former surface waves exist in semi-infinite homogeneous isotropic media with a stress-free boundary. In our present work, we consider plates whose thickness is much larger than the wavelength of the surface wave, which are akin to Rayleigh waves. When we make the geometric transform in the Navier equations, the stress-free boundary conditions also undergo the mapping. Hence one has to apply the transformation to the Navier Equations coupled with the stress-free boundary condition

$$\begin{cases} \frac{\partial}{\partial x_i} \left(C_{ijkl} \frac{\partial}{\partial x_k} u_l \right) + \rho_{jl} \omega^2 u_l = 0, \\ \mathbf{n} \cdot (\mathbb{C} : \nabla \mathbf{u}) = 0 \quad \text{on the boundary} \quad z = z_0, \end{cases} \quad (9)$$

with \mathbf{n} the (outward) normal at the points on the surface $z = z_0$. In our case, the horizontal plane $z = z_0$ stands for the soil-air interface of the thick plate. In the resulting Willis-type equations discussed in the previous sections, the approximated technique is again applied coupled with

$$\mathbf{n}' \cdot (\mathbb{C}' : \nabla' \mathbf{u}) = 0 \quad \text{on the boundary} \quad z = z_0, \quad (10)$$

where \mathbf{n}' is the normal at the image points.

2. Numerical implementation of Rayleigh-like waves in thick plates with soil parameters using Finite Element Method

Aiming at applications particularly in civil engineering such as seismic protection, we base the numerical model corresponding to the cloak described above on soil parameters. Namely, we use the Lamé coefficients $\lambda = 87.7 * 10^6$ Pa, $\mu = 58.5 * 10^6$ Pa and density $\rho = 1800$ kg/m³. The cloak consists of a vertical cylindrical hollow region of height 33.2 m, with an annulus-like basis of inner and outer radii $r_1 = 10$ m and $r_2 = 21.6$ m respectively and the z -axis as its main axis. It surrounds a homogeneous isotropic cylindrical domain of radius r_1 (the cloaked region) made of soil. Likewise, the cloak itself is located inside a cylindrical homogeneous isotropic medium (the ambient space) also made of soil and surrounded by a cylindrical shell of inner and outer radii $r_3 = 50$ m and $r_4 = 66.6$ m respectively, which is filled with an anisotropic heterogeneous absorptive medium acting as a (reflectionless) perfectly matched layer (PML). The top plane $z = 16.7$ m is a stress-free surface which is the interface between the soil and the air.

The implementation of this model in the finite element package COMSOL MULTIPHYSICS requires the use of Cartesian coordinates. Fortunately, 40 of the 3^4 spatially varying entries of the transformed elasticity tensor vanish identically. We mesh the computational domain using 1462046 tetrahedral elements, 54726 triangular elements, 1660 edge elements and 41 vertex elements.

A point force located at (8.3m, 36.7m, 16.7m), - that is, it lies on the soil-air free surface at a distance of 37.6 meters from the axis of the cloaked region, - oriented along the direction (0, 0, 1) generates a Rayleigh-like wave at frequencies 5.5 Hz (Fig 3 (A)) and 7.9 Hz (Fig 3 (B)). Following predictions in [24], one expects that some Rayleigh-like waves

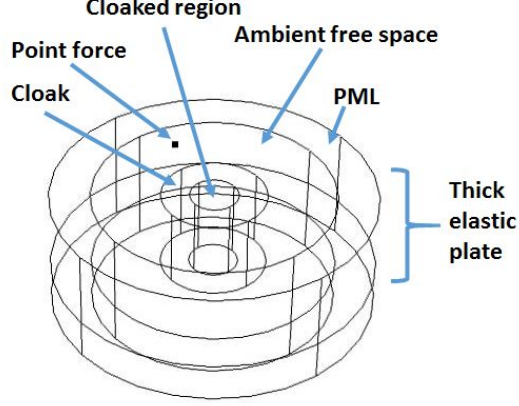


Figure 2: Geometric construction of the computational domain with a cylindrical Willis-like cloak surrounding a cylindrical region and a cylindrical annulus of PML to minimize wave reflections on the vertical boundary of the domain (the top boundary is stress-free everywhere).

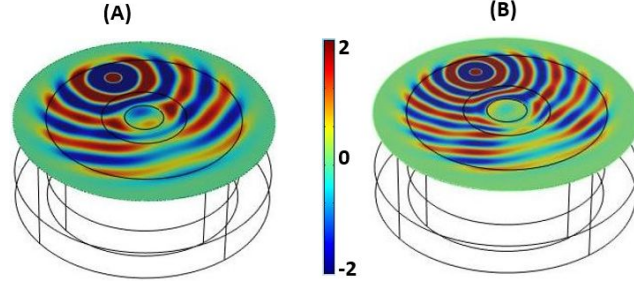


Figure 3: Out of plane component u_z of the displacement field $\mathbf{u} = (u_r, u_\theta, u_z)$ generated by a point force vibrating at frequency (A) $f = \omega/(2\pi) = 5.5$ Hz in panel (A) and $f = 7.9$ Hz in (B), polarized along z , which is located at the air-soil interface and at a distance $r = 0.2256$ m, from the axis of an approximated Willis cloak of inner radius $r_1 = 10$ m and outer radius $r_2 = 21.6$ m. One notes that the displacement field nearly vanishes in the invisibility region at the center of the cloak in panel B, whereas the amplitude and phase of the wave are nearly unperturbed outside the cloak. Such a seismic cloak for Rayleigh waves would protect a building placed in its center and have no impact on the surrounding buildings, unlike for a seismic shield like in [13] which would have disastrous effect for buildings facing reflected waves. However, as already noted in [24], at certain frequencies corresponding to a countable spectrum of the stress-free cavity, trapped modes exist that would have an antagonistic effect, see panel A. This is reminiscent of trapped modes unveiled by the group of Greenleaf [25] in the context of quantum cloaks.

generated by specific frequencies of the source will create resonances (trapped modes) within the cloaked region as in Figure 3 (A), wherein a dipole mode can be observed (the inner cylinder wobbles) : This occurs at a countable set of eigenfrequencies corresponding to the problem of the Neumann (stress-free) cylindrical cavity in the center of the cloak. At a source frequency away from the cavity trapped modes, one can clearly see that we achieve a good seismic protection (Fig 3 (B)). Such results for a cloak with a Willis-like heterogeneous anisotropic transformed medium are undoable in practice. We therefore present in the sequel a homogenization route towards achievable Willis-like seismic cloaks.

At this stage, let us point out that an alternative route to control of Rayleigh waves consists in applying tools of conformal optics as proposed by Ulf Leonhardt [18], that in the context of transformational elastodynamics lead to spatially varying isotropic elastic parameters [19]. Although this might seem an easier way towards cloaking, this requires structuring soil with pillars softer than soil, which is simply the opposite case to what we do in the sequel.

IV. HOMOGENIZATION APPROACH FOR APPROXIMATE WILLIS MEDIUM WITHOUT RANK-3 AND RANK-2 TENSORS

. Our homogenization approach to achieve required rank-4 and rank-2 tensors proceeds in two steps. Firstly, we follow the proposal the proposal of Greenleaf and coworkers [20] to apply the two-scale convergence method of G. Allaire and G. Nguetseng [21, 22] in the design of approximate multi-layered cloaks, we derive a set of effective

parameters for a multi-layered elastic cloak, which is akin to homogenized parameters obtained by the G-convergence approach in [23], except that these parameters remain dependent upon the macroscopic variable. We consider an alternation of concentric layers of respective elasticity tensors \mathbb{C}_1 and \mathbb{C}_2 and of respective densities ρ_1 and ρ_2 so that the overall elasticity tensor and density can be written

$$\begin{aligned}\mathbb{C}_\eta(\mathbf{x}) &= \mathbb{C}_1(\mathbf{x})1_{[0,1/2]}(\frac{r}{\eta}) + \mathbb{C}_2(\mathbf{x})1_{[1/2,1]}(\frac{r}{\eta}) \\ \rho_\eta(\mathbf{x}) &= \rho_1(\mathbf{x})1_{[0,1/2]}(\frac{r}{\eta}) + \rho_2(\mathbf{x})1_{[1/2,1]}(\frac{r}{\eta})\end{aligned}\quad (11)$$

where \mathbf{x} is the position vector, and $r = \|\mathbf{x}\| = \sqrt{x_1^2 + x_2^2}$ is its Euclidean norm and 1_I is the indicator function of the interval I (I is typically the unit cell size along the direction of periodicity). The spatially varying tensor \mathbb{C}_η is periodic on $I = [0, 1]$ and η defines the periodicity (the thinner the layers, the smaller η , the larger the number of layers). The governing equation reads:

$$\text{div}(\mathbb{C}_\eta(\mathbf{x}) : \nabla \mathbf{u}_\eta(\mathbf{x})) + \rho_\eta(\mathbf{x})\omega^2 \mathbf{u}_\eta(\mathbf{x}) = \mathbf{0} \quad (12)$$

When η tends to zero, it is shown in [23] that the solution \mathbf{u}_η to the above Navier equation two-scale converges towards \mathbf{u}_0 solution to the homogenized Navier equation:

$$\text{div}(\mathbb{C}_0(\mathbf{x}) : \nabla \mathbf{u}_0(\mathbf{x})) + \rho_0(\mathbf{x})\omega^2 \mathbf{u}_0(\mathbf{x}) = \mathbf{0} \quad (13)$$

with an effective (symmetric) elasticity tensor

$$\begin{aligned}2\xi \cdot \mathbb{C}_0(\mathbf{x})\xi &= \xi_{11}^2 (2 \langle \mu \rangle(\mathbf{x}) - 4 \langle (\mu - \bar{\mu})^2 / (2\mu + \lambda) \rangle(\mathbf{x})) - 4\xi_{11} \text{tr}\xi \langle (\mu - \bar{\mu})(\lambda - \bar{\lambda}) / (2\mu + \lambda) \rangle(\mathbf{x}) \\ &\quad + (\text{tr}\xi)^2 (\langle \lambda \rangle(\mathbf{x}) - \langle (\lambda - \bar{\lambda})^2 / (2\mu + \lambda) \rangle(\mathbf{x})) + 4 \langle \mu^{-1} \rangle^{-1}(\mathbf{x}) \xi_{12}^2 + 2 \langle \mu \rangle(\mathbf{x}) \xi_{22}^2\end{aligned}$$

where

$$\bar{\mu} = \left\langle \frac{\mu}{2\mu + \lambda} \right\rangle(\mathbf{x}) \left\langle \frac{1}{2\mu + \lambda} \right\rangle^{-1}(\mathbf{x}), \quad \bar{\lambda} = \left\langle \frac{\lambda}{2\mu + \lambda} \right\rangle(\mathbf{x}) \left\langle \frac{1}{2\mu + \lambda} \right\rangle^{-1}(\mathbf{x}) \quad (14)$$

and $\langle f \rangle(\mathbf{x}) = \langle f(\mathbf{x}, \mathbf{y}) \rangle := \int_Y f(\mathbf{x}, \mathbf{y}) d\mathbf{y}$ with Y the unit cell.

Moreover, the effective density reads as

$$\rho_0(\mathbf{x}) = \langle \rho \rangle(\mathbf{x}). \quad (15)$$

One notes that the effective density is thus scalar valued and cannot achieve a rank-2 symmetric elasticity tensor as required by the approximate Willis medium constituting the cloak. Inspired by earlier work on locally resonant acoustic metamaterials for anisotropic effective density, we therefore add a second step in the homogenization process, that amounts to adding concrete bars in the soil.

V. ELASTIC THICK PLATES STRUCTURED WITH CONCRETE COLUMNS FOR HOMOGENIZED WILLIS MEDIUM WITHOUT RANK-3 TENSORS BUT ANISOTROPIC EFFECTIVE DYNAMIC DENSITY

In this section we investigate the case of seismic cloaks which are a mitigation of cylindrical elastodynamic cloaks as proposed in [29] for in-plane coupled shear and pressure waves (which unfortunately require Cosserat media) and thin plate cloaks [30–34] for Lamb waves. Our case is indeed dedicated to Rayleigh like waves in thick plates. We do not claim that our cloaks work for body waves.

Bearing in mind that many authors have thus far achieved dynamic anisotropic density, see for instance [26–28], symmetrized Willis cloaks are then achievable by classical homogenization approaches (getting rid of rank-3 tensors) with high contrast in material parameters for the artificial anisotropic density.

We would like to explore the propagation of elastodynamic waves in two types of cloaks that are in line with such a high-contrast homogenization, using the finite element method. The two cloaks are dedicated to seismic protection and could be achieved by manufacturing soil using concrete columns. Physical parameters are $\lambda = 87.7 * 10^6$ Pa, $\mu = 58.5 * 10^6$ Pa and density $\rho = 1800$ kg/m³ for soil and $\lambda = 18.24 * 10^9$ Pa, $\mu = 9.39 * 10^9$ Pa and density $\rho = 2300$ kg/m³ for concrete.

In order to prevent eventual reflections on the boundaries, Perfectly Matched Layers (PMLs) are applied to simulate infinite media. A point source is placed atop a semi infinite medium representing the earthquake epicenter, which provoke a Rayleigh-like wave (a type of wave that can be harmful and detrimental for buildings). The outside and

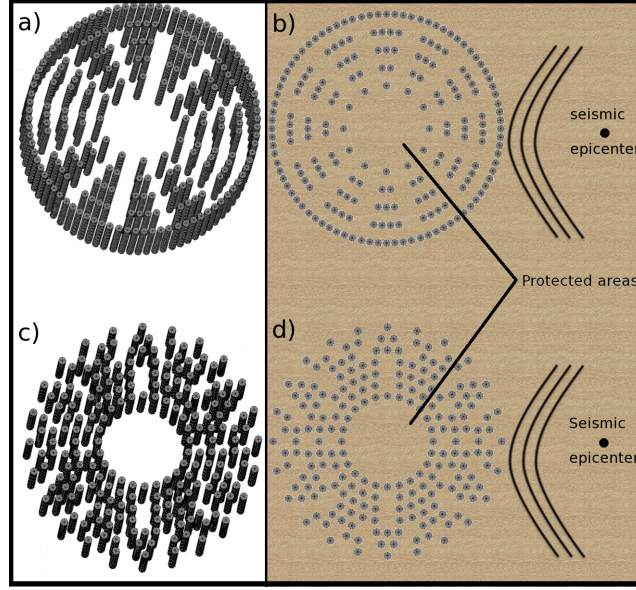


Figure 4: Schematic illustration of the homogenized cloaks a), c) under a 3D view and b), d) top view after being implemented in soil basin.

inside boundaries of the cloak measure $30m$ and $10m$, respectively. The point source is located at $50m$ from the cloak core. Concrete columns have $2m$ of diameter and penetrates $30m$ in depth. The soil depth is set to $50m$ and we apply free traction boundary condition to the background. We assume that such condition gives comparable results to those that might be obtained if the bedrock is identified beneath soil. Indeed, potential reflection occur in both cases due to impedance mismatch. We deliberately consider such configuration that is more realistic rather than call upon PML. Concrete columns are arranged in a way that the effective density decreases we move towards the center of the cloak. The simulation was optimized enough to meet the seismic issues reality. Indeed, the range of frequency gives rise to wavelengths much larger than the columns diameters (subwavelength approximation to valid the homogenization theory) and enough small compared to the basin depth to investigate Rayleigh waves rather than plate waves. Furthermore, we notice that the arrangement is coherent with the formula of the density of the transformed media previously reported by [30] and reads:

$$E_r = \left(\frac{r - r_1}{r} \right)^2, \quad E_\theta = \left(\frac{r}{r - r_1} \right)^2, \quad \text{and} \quad \rho = \alpha^2 \left(\frac{r - r_1}{r} \right)^2, \quad (16)$$

with $\alpha = \frac{r_2}{r_2 - r_1}$. However, this step doesn't achieve the effective anisotropy.

We depict in figure 2 the real part of the out of plane displacement field in 3D and top view representations at 5.5 Hertz. It is observed that more than 50% of the field is suppressed at the center of the cloak (zone of protection) but recovered at its exit. The acceleration phenomenon is also noticed within the cloak area due to the higher effective Young's modulus.

The cloak is found to be efficient between 4.5 Hz and 6.5 Hz for the two cloaks that has been tested. It is worth noting that the lower limit (4.5 Hz) is inwardly connected to the basin depth and the upper limit (6.5 Hz) to the diameter of the columns. The smaller is the diameter the higher is the upper frequency limit. Indeed the phenomenon is constrained by the diffraction that might be caused by the columns.

We tested as well the other configuration in which the inward effective anisotropy is increased. This is accompanied by an undesirable reduction of the effective density the outer boundary of the cloak. This can be explained as the following: the concrete columns are arranged by bunch of clusters with one element over the first layer, two elements over the second and so forth up to the sixth layer. The seventh and last layer is isotropic and could be seen as a seismic shield. We depict in figure 4 the real part of the out of plane displacement field in 3D and top view representations at 5.5 Hertz. For sake of comparison, the free medium is also represented. We can notice that unlike the first configuration, there is much less reflection at the cloak entrance (due to the smooth mismatch of impedance), a quasi perfect restitution of the field at the exit and a comparable protection inside the cloak (almost 50% of the energy is suppressed).

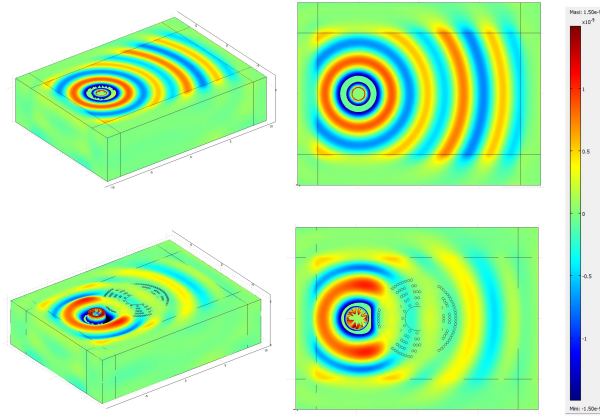


Figure 5: 3D and top views of the out of plane displacement field ($\text{Re}(u_z)$) at 5.5 Hz of wave propagating atop a free medium (upper panel) and within a surface manufactured with cloak of type I. One notes that the wave wavefront is nearly unperturbed by the cloak, but its amplitude is decreased within the center of the cloak.

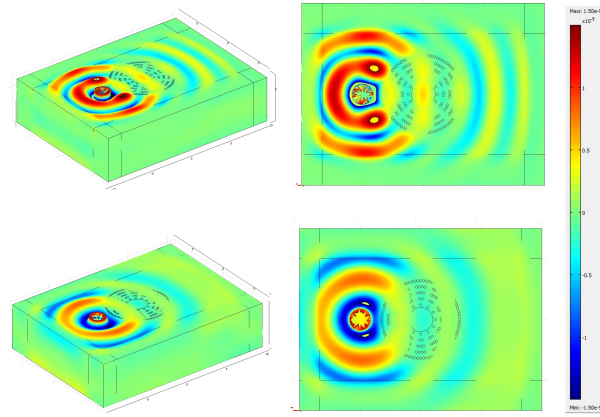


Figure 6: 3D and top views of out of plane displacement field ($\text{Re}(u_z)$) at 6.5 Hz (upper panel) and 4.5 Hz (lower panel). One notes that the wave wavefront is nearly unperturbed by the cloak, but its amplitude is nearly suppressed within the center of the cloak in the lower panel.

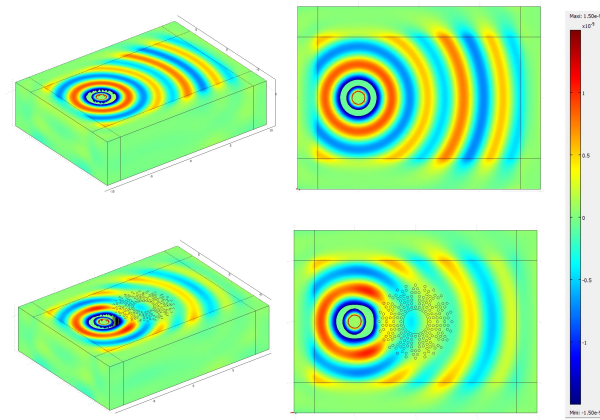


Figure 7: Same as figure 5 with soil structured by a cloak of type II.

VI. CONCLUDING REMARKS

In this article, we have conclusively shown that transformed Navier equations of the Willis type with a symmetric transformed elasticity tensor, allows for approximate cloak's designs getting rid of the rank-3 transformed tensors unveiled in [14]. A further approximation consists in structuring soil with buried concrete pillars judiciously placed (note that this is the opposite case to what is proposed in [19], wherein soil was structured with softer columns. This is done and finite element computations confirm the cloaking efficiency (invisibility and protection) of two types of large scale seismic cloaks within a soft elastic plate (with soil parameters). Indeed, the two designs we propose allow one to considerably reduce the the elastic field vibrations in the center of the cloak with virtually no disturbance of the wave field outside the cloak. The protection could be further improved using the concept of mixed cloak [24], which amounts to adding a PML layer at the inner boundary of the cloak, in essence some absorptive anisotropic medium. We would like to add that our results could be translated into geophysics upon use of time domain computations, for instance with specfem software. It would be also important to study the effect of viscoelasticity on the elastic wave propagation, which can be done with comsol multiphysics. Finally, some implementation of the seismic cloak with subsequent field test are in progress with the Ménard company.

A.D., Y.A. and S.G. acknowledge European funding through ERC Starting Grant ANAMORPHISM.

-
- [1] A. Diatta and S. Guenneau, 'Controlling solid elastic waves with spherical cloaks', *Appl. Phys. Lett.* 105, 021901 (2014).
 - [2] E. Cosserat, F. Cosserat, 'Theory of deformable bodies', Scientific Library A. Hermann and Sons, Paris (1909).
 - [3] S. Brûlé and E. Javelaud, 'Could deep soil densification impact the seismic site effect?', in *Proceedings of the 9th Annual International Conference on Urban Earthquake Engineering* (Tokyo Tech CUEE, Tokyo, 2012), 497-501 (2012).
 - [4] Y. Achaoui, B. Ungureanu, S. Enoch, S. Brûlé, S. Guenneau, 'Seismic waves damping with arrays of inertial resonators,' *Ext. Mech. Lett.* (<http://dx.doi.org/10.1016/j.eml.2016.02.004>).
 - [5] J.F. Semblat and A. Pecker, 'Waves and vibrations in soils: earthquakes, traffic, shocks, construction works', IUSS Press, Pavia (2009).
 - [6] R.D. Woods, Screening of surface waves in soils, Tech. Rep. IP-804, University of Michigan (1968).
 - [7] P.K. Banerjee, S. Ahmad and K. Chen 'Advanced application of BEM to wave barriers in multi-layered three-dimensional soil media,' *Earthquake Eng. and Structural Dynamics* 16, 1041-1060 (1988).
 - [8] F. Meseguer, M. Holgado, D. Caballero, N. Benaches, J. Sanchez-Dehesa, C. Lopez, and J. Llinares, 'Rayleigh-wave attenuation by a semi-infinite two-dimensional elastic-band-gap crystal,' *Phys. Rev. B* 59, 12169 (1999).
 - [9] S. Benchabane, O. Gaiffe, G. Ulliac, R. Salut, Y. Achaoui and V. Laude, 'Observation of surface-guided waves in holey hypersonic phononic crystal,' *Appl. Phys. Lett.* 98 (17), 171908 (2011).
 - [10] Y. Achaoui, A. Khelif, S. Benchabane, L. Robert and V. Laude, 'Experimental observation of locally-resonant and Bragg band gaps for surface guided waves in a phononic crystal of pillars,' *Phys. Rev. B* 83 (10), 104201 (2011).
 - [11] A. Khelif, Y. Achaoui, S. Benchabane, V. Laude, B. Aoubiza, *Phys. Rev. B* 81 (21), 214303 (2010).
 - [12] Y. Achaoui, A. Khelif, S. Benchabane, V. Laude, *J. Phys. D: Appl. Phys.* 43, 185401 (2010).
 - [13] S. Brûlé, E. Javelaud, S. Enoch and S. Guenneau, 'Experiments on seismic metamaterials: Molding surface waves,' *Phys. Rev. Lett.*, 112 (13), 133901 (2014).
 - [14] G.W. Milton, M. Briane, and J.R. Willis, 'On cloaking for elasticity and physical equations with a transformation invariant form,' *New J. Phys.* 8, 248 (2006).
 - [15] A.N. Norris and A.L. Shuvalov, 'Elastic cloaking theory,' *Wave Motion* 48, 525-538 (2011).
 - [16] J.R. Willis, 'Variational principles for dynamic problems for inhomogeneous elastic media,' *Wave Motion* 3, 1-11 (1981).
 - [17] J.B. Pendry, D. Schurig and D.R. Smith, 'Controlling Electromagnetic Fields,' *Science* 312 1780 (2006).
 - [18] U. Leonhardt, 'Optical Conformal Mapping,' *Science* 312, 1777 (2006).
 - [19] A. Colombi, S. Guenneau, P. Roux, R.V. Craster, 'Transformation seismology: composite soil lenses for steering surface elastic Rayleigh waves,' *Scientific reports* 6, 25320 (2016).
 - [20] Greenleaf, A., Kurylev, Y., Lassas, M. and Uhlmann, G. 'Isotropic transformation optics: approximate acoustic and quantum cloaking,' *New J. Phys.* 10, 115024 (2008).
 - [21] Nguetseng, G. A general convergence result for a functional related to the theory of homogenization. *SIAM J. Math. Anal.* 20, 608623 (1989).
 - [22] Allaire, G. Homogenization and two-scale convergence. *SIAM J. Math. Anal.* 23, 1482-1518 (1992).
 - [23] V.V. Jikov, S.M. Kozlov and O.A. Oleinik, *Homogenization of Differential Operators and Integral Functionals*, Springer-Verlag Berlin Heidelberg (1994).
 - [24] A. Diatta and S. Guenneau, 'Elastodynamic cloaking and field enhancement for soft spheres,' *J. Phys. D: Appl. Phys.* (2016). In press.
 - [25] A. Greenleaf, Y. Kurylev, M. Lassas, G. Uhlmann, Approximate quantum cloaking and almost trapped states. *Phys. Rev. Lett.* 101, 220404 (2008)
 - [26] D. Torrent, A. Hakansson, F. Cervera, Sanchez-Dehesa, 'Homogenization of two-dimensional clusters of rigid rods in air,' *Phys. Rev. Lett.* 96, 204302 (2006).

- [27] D. Torrent, J.S. Dehesa, 'Anisotropic mass density by two-dimensional acoustic metamaterials,' *New Journal of Physics* 10 (2008) <http://iopscience.iop.org/article/10.1088/1367-2630/10/2/023004/meta>
- [28] H.H. Huang, C.T. Sun, Locally resonant acoustic metamaterials with 2D anisotropic effective mass density , *Philosophical Magazine* 91, 981 (2011). *Science* 314, 977-980 (2006).
- [29] M. Brun, S. Guenneau and A.B. Movchan, 'Achieving control of in-plane elastic waves,' *Appl. Phys. Lett.* 94, 061903 (2009).
- [30] M. Farhat, S. Guenneau, S. Enoch and A.B. Movchan, 'Cloaking bending waves propagating in thin elastic plates,' *Phys. Rev. B* 79, 033102 (2009).
- [31] M. Farhat, S. Guenneau and S. Enoch, 'Ultrabroadband Elastic Cloaking in Thin Plates,' *Phys. Rev. Lett.* 103, 024301 (2009).
- [32] M. Farhat, S. Guenneau and S. Enoch, 'Broadband cloaking of bending waves via homogenization of multiply perforated radially symmetric and isotropic thin elastic plates,' *Phys. Rev. B* 85, 020301 R (2012).
- [33] N. Stenger, M. Wilhelm and M. Wegener, 'Experiments on elastic cloaking in thin plates,' *Phys. Rev. Lett.* 108, 014301 (2012).
- [34] A. Colombi, P. Roux, S. Guenneau and M. Rupin, 'Directional cloaking of flexural waves in a plate with a locally resonant metamaterial,' *The Journal of the Acoustical Society of America* 137 (4), 1783-1789 (2015).